

Cooling and Suppression Phenomena of the Flames by Mixing of the High Speed Jet in the Engines and Their NO Reduction Mechanism

S.Matsuoka and G.Sugimoto*

Emeritus Professor

Tokyo Institute of Technology

2149-1, Hayama-Machi, Ittshiki, Miura-gun, Kanagawa 240-01

Japan

** Toyo Engineering Co.*

I SUMMARY, MOTIVATION and OBJECTIVE

Though it is known that the engines with jet flame from an auxiliary chamber such as an IDI diesel engine or a tri-valve SI engine have a low NO emission characteristics without sacrificing much efficiency, there have not been determined theories^(1~5) regarding the reason causing this. This paper that will clarify this reason is motivated from recent ecological requirements to elucidate and utilize the causative relationship of this phenomenon. By mere chance the authors hit up to adapt their theory of self-reintrainment of burned gas (REOBG) in the diesel flame verified by Matsoka⁽¹¹⁾ to this problem. This hint is that the flame of the jet of SI engine with pre-chamber will entraine and mix with the surrounding gas as well by the common phenomena as this REOBG, and cooled and NO is reduced. Therefore objective of this paper is to verify the aforesaid hint or hypothesis on this SI engine but also to discuss the similarity of the characteristics with the DI jet and also to investigate the possibility of a simultaneous reduction of fuel consumption, NO, and particulates by the flame cooling in DI engine.

II GAS ENTRAINMENT PHENOMENON BY MIXING IN THE TWO KINDS OF HIGH SPEED JETS

A: INTRODUCTION OF BURNED GAS RE-ENTRAINMENT THEORY IN THE DIESEL SPARY FLAMES^{(11,13),(14)}

In reference (11), one of the authors, S. Matsuoka proposed a hypothesis of the combustion suppression phenomenon by the surrounding burned gas self re-entrainment into the spray flame. They verified this theory using the 3 zone model as shown in Fig.1. This will be introduced briefly as follows.

A-1 3 ZONE MODEL AND AMOUNT OF ENTRAINED GAS

Combustion chamber is divided each uniform 3 zones

(Numbers in parentheses designate References at end of paper.)

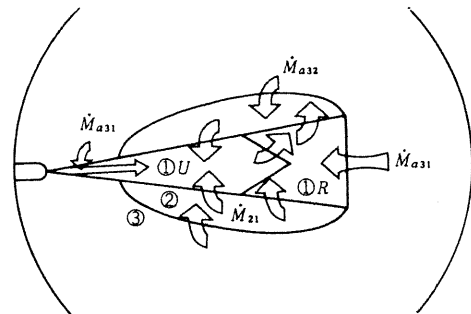


Fig.1. Schema of 3 Zone Model of Free Spray in RCM^(11,13,14)

Zone 1: unburned fuel & air mixture + reentrained burned gas.
Zone 2: burned gas + entrained air.
Zone 3: air.

as shown in Fig.1. The composites of each zone are explained in the figure. The necessary condition of the analytical model of this 3 zone model is satisfied by adding one assumption of a stratified constant. The measured data are ROHR, ROI, Rate of Air Entrainment, Air amount etc.. The equation of the mass flow rate of the entrained gas in ref. (11) \dot{M}_{mix} is fundamentally based on the equation of Khan⁽¹⁰⁾. Further improvements are made and equation (1) by considering the temperature-viscosity co-efficient C_v and inert gas dilution co-efficient $W_{in\bar{s}}^m$ according to the authors' REOBG Theory⁽¹¹⁾ is proposed⁽¹³⁾⁽¹⁴⁾ as follows.

$$\dot{M}_{mix} = C_m (T_u/T_1)^{C_v} (1 - W_{in\bar{s}}^m) \cdot M_{uf} \cdot V_s \quad (1)$$

\dot{M}_{mix} : mass flow rate of mixed fuel

M_{uf} : unburned fuel mass

V_s : spray tip velocity

T_1 : initial mixture temperature before mixing

T_u : gas temperature after mixed

C_m : mixing coefficient

m : minus effect coefficient of inert gas

C_v : temperature coefficient

$W_{in\bar{s}}$: mass ratio of inert gas

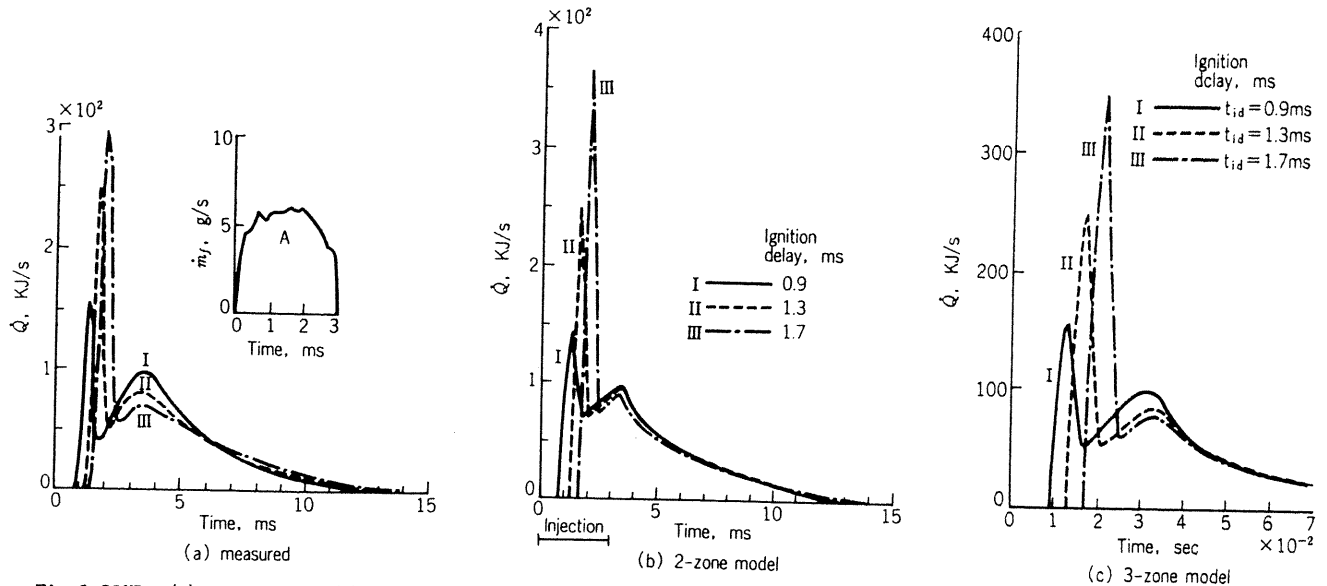


Fig. 3. ROHRs, (a) Measured, (b) Calculated in 2 Zone and (c) in 3 Zone Model, when Ign.-Delay is varied^(11, 13, 14).

A-2 AN INVESTIGATION ON THE CALCULATED RESULTS

Fig. 2 indicates only the diffusion portions of 2 & 3 zone models using same constants. From the results of this and others, ROHRs of calculated ones in Fig. 3 are obtained. They show good agreement in case of 3 zone model with measured ROHR. In these figures, the decrease of ROHR in case of 3 zone model is obvious when it compared with the conventional 2 zone model. This clearly demonstrates the importance of the consideration of the entrainment of the surrounding gas.

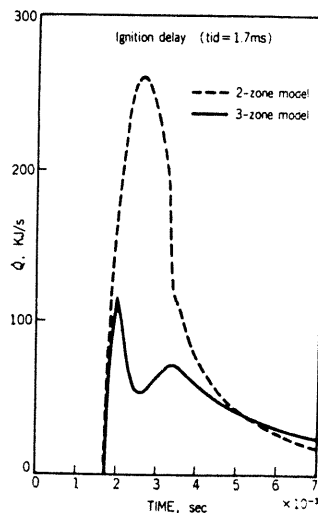


Fig. 2. Pred-ROHR of only the Diffusion Portions when Ign.-Delay is 1.7ms case, by 2 & 3 Zone Model⁽¹⁴⁾.

B ; COOLING PHENOMENON BY MIXING OF THE JET FLAME IN THE SI ENGINE WITH PRE-CHAMBER

B-1 Experimental Engine and the Measured Data Employed

The specifications of the employed engine (6, 7, 8) are listed as follows.

Engine type: 4 cycle mono cylinder with pre-chamber gasoline engine

Valve mechanism: SOHC-3 valves, **Displacement:** 454 c.c.

Bore \times Stroke: 85 \times 80 cm.

Volume of sub-chamber: 13% of clearance volume

Connecting orifice bore: 4, 6, 9, 12, 20 ϕ mm

The measured data, calculations and photographs are

mostly referred from references (6), (7), (8), (9), (11), (12), (13), (14).

B-2 Predictions of the Jet Flow Temperature and NO Emission Rate by the Conventional Model

B-2-1 Combustion Model and Temperature Calculation Process

1) Calculation Process; Combustion chamber is divided by 30 elements in a divided element model. The boundary condition of non-uniform temperature zone is given as following 3). Burning rate is given by true pressure as following 2). Local flame temperature is calculated by deducting each wall heat loss shown in Fig. 4⁽⁷⁾ left side at each element by element in temperature calculation which obtained from true pressure.

2) True pressure diagrams; This is obtained from measured pressure diagram adding total wall heat loss shown in Fig. 4⁽⁷⁾ right side.

3) Geometry of flame and surface area; In the main chamber calculated volume burned ratio and geometry of flame shown in B-3-2-2 are given and wall contact area-velocity and flame area are obtained as shown in Fig. 5.

4) Consideration of physical properties; The thermal dissociation and the physical properties are all taken into account.

B-2-2 Comparison with the Predicted and the Measured Data and their Investigation.

1) Flame temperature chart of each element of jet; Dotted and real lines in Fig. 6 are calculated by divided element method by wall heat loss is considered and not.

2) A comparison and investigation with predicted and the measured results: Even the factors

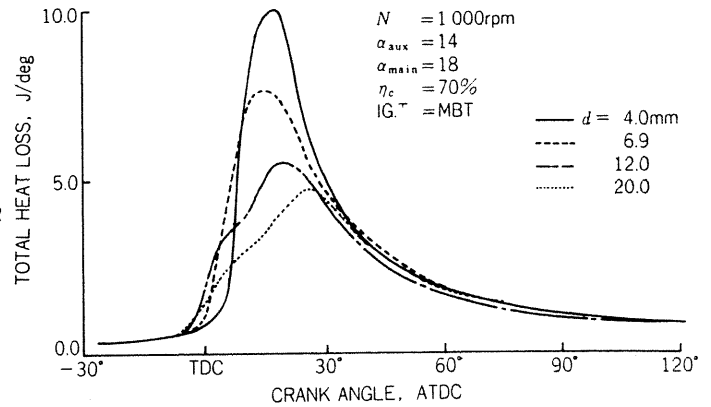
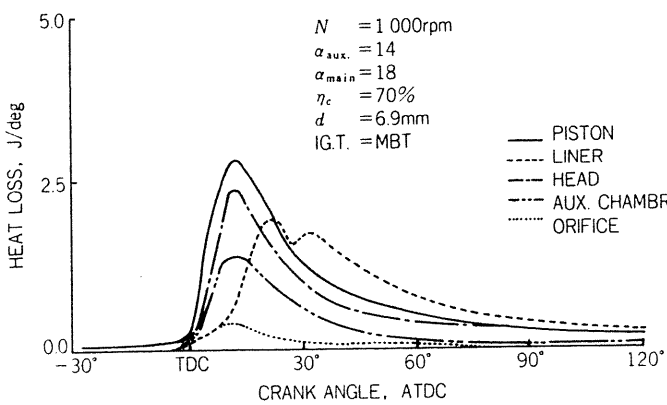


Fig.4. Measured Heatloss of Combustion Chamber (MBT) (7) left ; at each part ($\phi 6.9\text{mm}$). right; at total, when bore of orifices are varied (MBT).

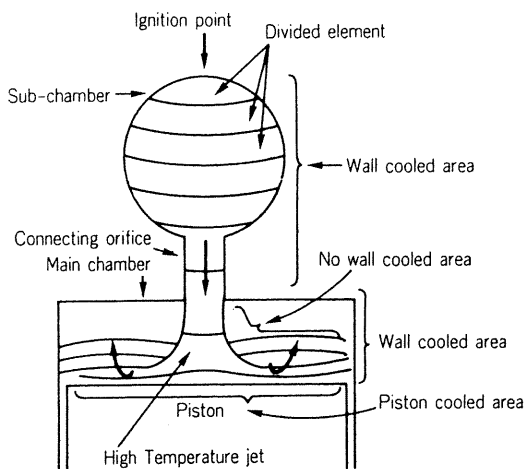


Fig.5. Schema of Jet Flow, Flame Propagation and Flame Contact Area with Wall in the Tri-Valve SI Engine with Pre-Chamber .

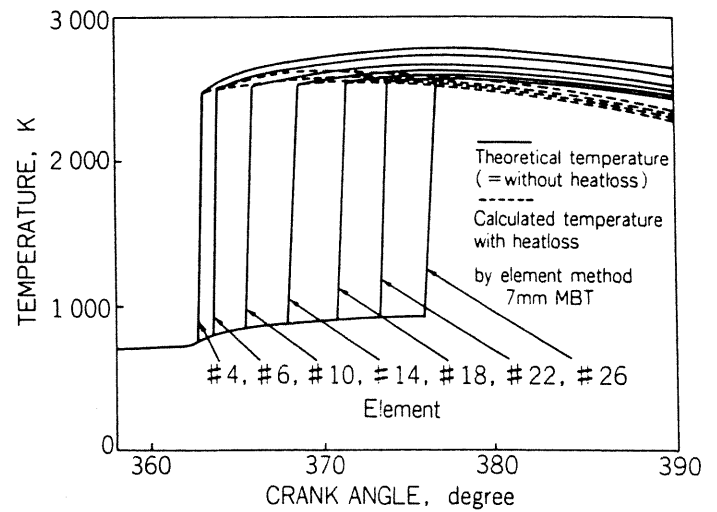


Fig.6. Pred-Temperature at each Element by Divided Element Method, when considered with and without Heatloss ($\phi 7\text{mm}$, MBT).

influencing on jet flame temperature as conventional as mentioned in B-2-1 are taken into consideration, the calculated flame temperature of the most of elements is in the range of 26~2700K as shown in Fig.6. These results far exceed the measured optical temperature of 2500K about 100~200K as shown in Fig. 9 . It is clear that from these predicted flame temperatures, the prediction of measured 1,000ppm level of NO as shown in Fig.14 can never be expected. It is imagined that some ignorance in temperature prediction existed. This suggests that the cause of the flame temperature reduction of an engine with an auxiliary chamber and the resulting decrease in the NO emission amount can not be only resoned by the wall heat loss.

B-3 New Concept of Gas Entrainment, Mixing, and Cooling Phenomena

B-3-1 Explanation of the New Concept of Flame Propagation and Cooling Phenomena by Mixing

In this new concept, the jet flow rapidly increases its flame propagating surface area propelled by its

high velocity, strong momentum and turbulence. Therefore it entrains the surrounding frontal low temperature lean unburned gas including much excess air while mixing with its own high temperature, high specific heat burned gas, that is so called inner EGR to form a flame zone as indicated in Fig.7.

B-3-2 Presentation of the Conception

A schema of this concept is indicated in a model form in Fig 7. This is expressed in the following 1), 2) and 3).

1) The Entrainment and Mixing Amount.

\dot{M}_R of the mass flow rate of the mixture is deduced from equation (1) as follows.

$$\begin{aligned} \dot{M}_R &= C_m (T_u/T_1)^{C_v} (1 - W_{in\bar{z}}^m) \cdot V \cdot A \cdot B_R \\ &= C_m (T_u/T_1)^{C_v} (1 - W_{in\bar{z}}^m) \cdot V^2 \cdot A \cdot C_f \end{aligned} \quad (2)$$

- \dot{M}_R : mass flow rate of jet flow mixture
- A : surface area of jet flow
- V : jet velocity
- B_R : turbulence rate of jet = $V \cdot C_f$
- C_f : turbulence coefficient

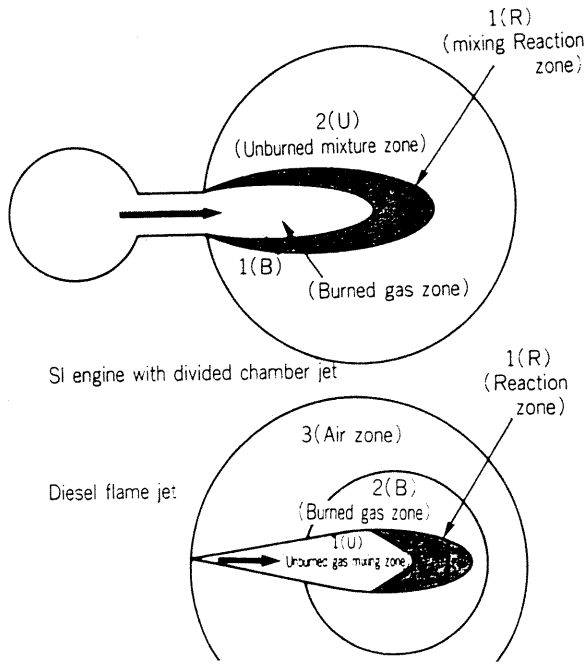


Fig 7. Schema of Cooling Phenomenon by Mixing, in Jet of SI engine with Pre-Chamber and in DI Diesel flame Jet.

2) Investigation of the Flame Propagation Pattern, Surface Area

From the high speed schlieren shadow photography taken from ref. (12), a simplified model is drawn as shown in Fig 8(A,B), and the flame surface area A and wall contact position etc. are obtained.

3) Flame Temperature of Cooling Phenomenon by Mixing

This is expressed as follows:

$$T_R = T_b + \Delta T$$

$$\Delta T = (M_R h_{b,u,a} + Q_{uf}) / M_R C_{p,b,u} \quad (3)$$

- $h_{b,u,a}$: average enthalpy of entrained burned gas and unburned air into flame zone
- $C_{p,b,u}$: average constant pressure specific heat of entrained burned and unburned mixture
- Q_{uf} : calorific value of entrained unburned fuel

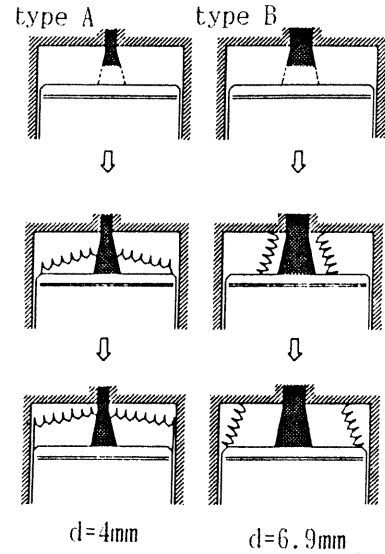


Fig. 8 Flame Propagation Model, type A in 4mm (left), type B in 6.9 mm Orifice Bore (right).

- ΔT : temperature variation caused by mixing entrainment combustion
- T_b : initial temperature of mixture before combustion
- T_R : flame temperature after mixing combustion

B-4 Flame Temperature and NO Emission Rate under New Concept

B-4-1 Comparison of the Optical Measured Data by Absorption-Radiation Method with Calculated Result

Comparisons of flame temperature with the measured data in the reference (8) as shown in Fig.9 and by the calculations in Fig.12 are made at -10° ATDC ignition timing each. These indicate that in the case of a 4mm bore the maximum temperature on the optical path across the jet flow measured by 4.8μ wavelength is 2350K and by calculation is 24~2300K at # 6, 10 elements, all at $+10^\circ$ ATDC position. In the case of a 6.9mm bore, the measured temperature is 2490K and calculated temperature is 2450~2350K each and both are higher than the 4mm case. Both measured and calculated temperature mostly coincide together as shown above.

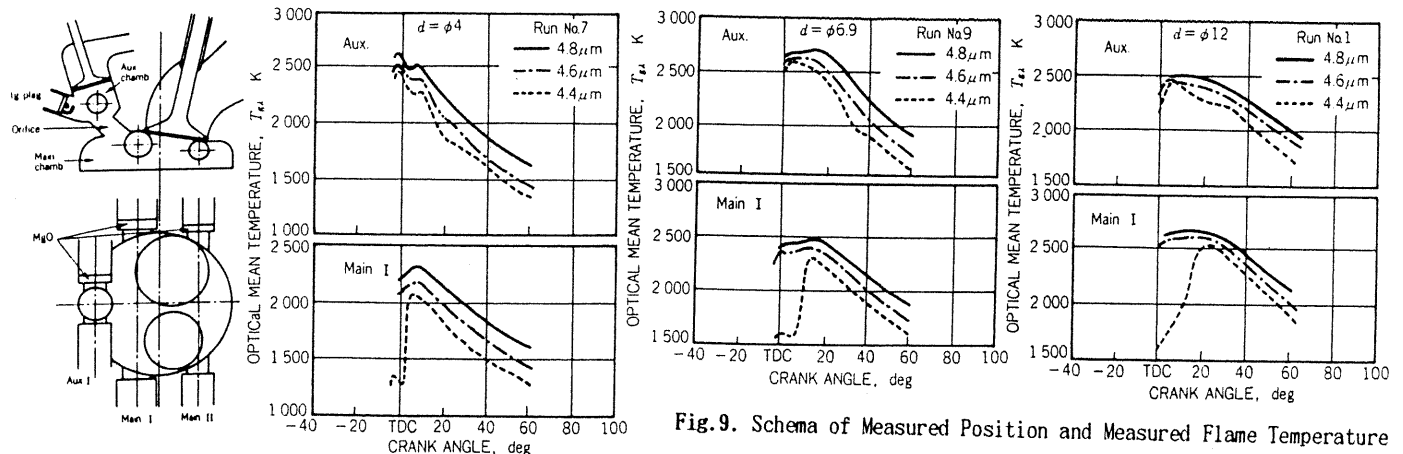


Fig. 9. Schema of Measured Position and Measured Flame Temperature

by Absorption-Radiation Method at aux-chamb. and Main-Chamb. using $4.8\sim 4.4\mu$ wavelength⁽⁸⁾ (orifice bore: 4, 6.9, 12mm).

B-4-2 Comparison of the Effects of the Ignition Timing Variation

1) In the case of fixed ignition timing at -10° ATDC in Fig. 14, NO emission is higher at 4mm bore case than 6.9mm bore and also it is higher than in MBT case. The reason to cause of these are, at the former case that is needless to say due to their faster jet velocity at 4mm bore. Also additionally cooling phenomenon by mixing is much deadend by their recovery of temperature at the latter period as shown in Fig. 12, 13. In the case when compared with MBT case, timing of this case is much faster than also NO increases.

2) In the MBT case: As shown in Fig. 10, 11, the 10th element of 4 mm bore case shows about 150K drop in temperature than 7mm bore case and also its recovered temperature is about the same as 2500~500K

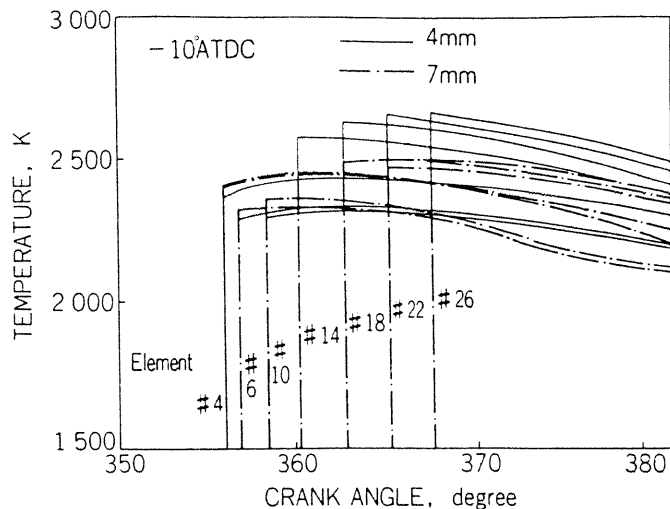


Fig. 12. Pred-Flame Temperature of each element, at ϕ 4mm and ϕ 6.9mm, each -10° ATDC case, when considering with heatloss+cooling phenomenon by mixing case.

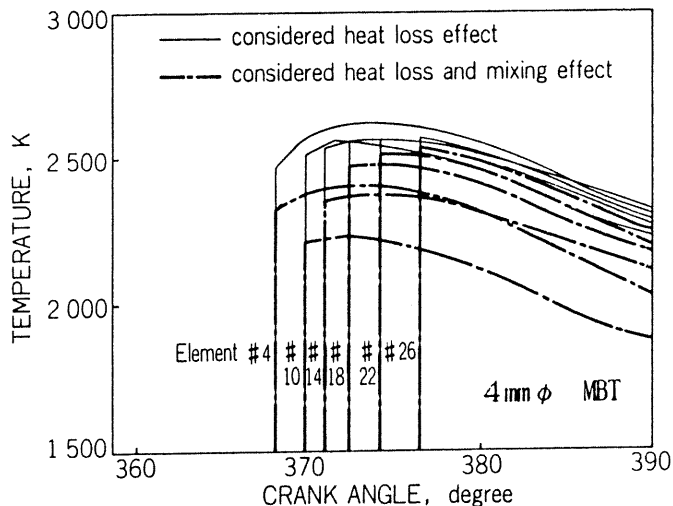


Fig. 10. Pred-Flame Temperature at ϕ 4mm, MBT case, when calculations are made considering with heatloss only case, with heatloss +cooling phenomenon by mixing case.

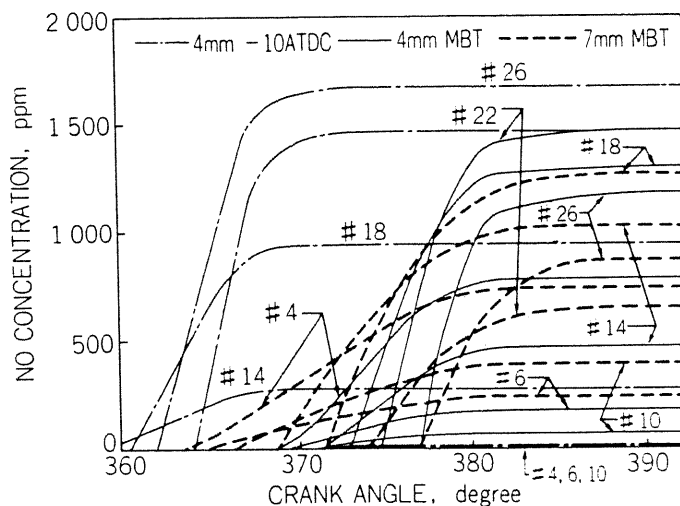


Fig. 13. Pred-NO Concentration in each element, at ϕ 4mm, -10° ATDC, MBT and ϕ 6.9mm, MBT, when considering the heatloss+cooling phenomenon by mixing.

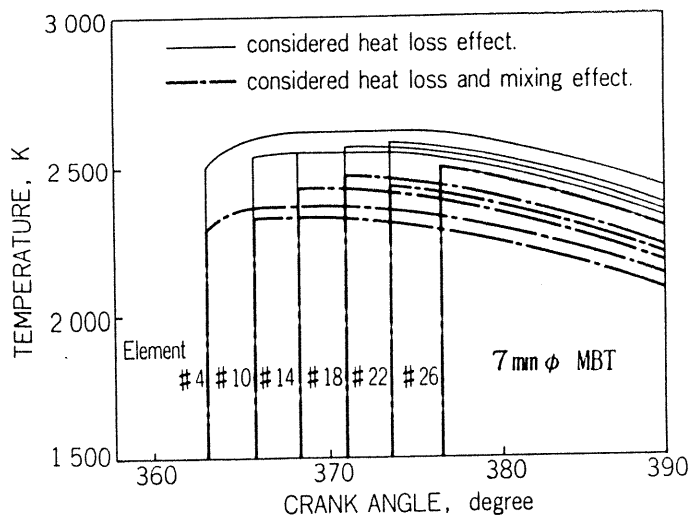


Fig. 11. Pred-Flame Temperature of each element at ϕ 6.9 mm, MBT case, when considering with heatloss only case, with heatloss + cooling phenomenon by mixing case.

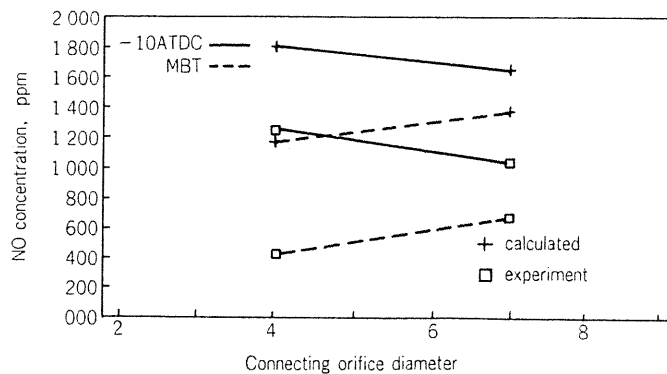


Fig. 14 NO Concentration in Exhaust by Measured and Calculated at MBT and -10° ATDC, Ign-Timing case.

in latter period. These trends are only explained by the cooling phenomenon by mixing in the jet. So that would be the reason of larger decrease of MBT NO emission in the 4mm than 7mm bore case as indicated in Fig 13,14.

III SIMILARITY DISCUSSION OF THE JET FLOW BETWEEN SI ENGINES WITH PRE-CHAMBER AND DI DIESEL ENGINES

III-1 Quantitative Discussion

At the comparison of mass flow rate of mixing of both jets, equation (1) of the unburned pre-mixture mixing rate in the pre-mixed combustion and equation (2) of the unburned fuel mixing rate in diffusion combustion are fundamentally, in this paper, constructed assuming to be equivalent each under highly turbulented conditions. From this, it is thought that both entrained mixing amounts are quantitatively similar.

III-2 Qualitative Discussion

A comparison is made between the structure of both flames. As indicated in Fig. 7, in the SI engine with pre-chamber, unburned and burned gas are located at the in and out side of pre-mixed flame zone. In contrast to this, in the spray diffusion flame case, the burned and unburned gas are located stratified at the same out side of flame zone. When the jet speed is enhanced, though the ratio of entrained burned and unburned gas amounts will be some different in each flame, the trends of ROHRs, the cooling or combustion suppression phenomena by mixing which are influenced by these will be not big different. But these details are unknown.

IV CONCLUSIONS AND NEW DIRECTIONS FOR THE REDUCTION OF NO CONCENTRATION

- 1) The low NO characteristics of a SI engine with pre-chamber is mainly caused by the cooling phenomenon originated by mixing of the jet flow from the pre-chamber. This hypothesis was verified by the good agreement between the theoretical calculation and the measured data of flame temperature and NO concentration.
- 2) As this phenomenon occurs in the initial burning portion, NO reduction is quite effective.
- 3) By the discussion of the similar characteristics at the both jets of SI in (1) and DI diesel, in the later case it is assumed that the strengthening of the air-entrainment rate by the spray flow will decrease the combustion suppression phenomenon and promote not only the combustion but also the cooling phenomenon in the same way as in case (1).
- 4) The cooling effect by jet flow is functioned by its velocity square and surface area by eq. (2). By strengthening these factors, as like micro-hole or rectangular hole, and utilizing these combustion and cooling characteristics in a diesel

spray flame, the simultaneous reduction of the three terms of fuel consumption, NO and particulate concentration will be achieved.

ACKNOWLEDGEMENT:

The authors wish to express their gratitude for the co-authors of the following references (6,7,8,11,12), which we used as the fundamental data of this paper. Also thanks are due to the Research Co-operative Committee-#86, #107 of JSME and to all the members of them.

REFERENCES

- (1) Yagi, K., Date, T., Inoue, K. "NOx Emission and Fuel Economy of the HONDA CVCC Engine" SAE Paper-741158, 1974.
- (2) Sakai, K., Kunii, S., Tsutsumi, S., Nakagawa, Y. "Combustion Characters of the Torch Ignited Engine" SAE Paper 741167, 1974.
- (3) Hires, S. D., Echian, A., Heywood, J. B., Tabaczynsky, R. J., Wall, J. C. "Performance and NOx Emission Modeling of a Jet Ignition Pre-Chamber Stratified Charge Engine" SAE Paper, 760161, 1976.
- (4) Asanuma, T., Babu, G., Yagi, S. "A Cycle Simulation of 3-Valve Stratified Charge Engines" T-JSME Vol. 45-395, 1979.
- (5) Konishi, M., Nakamura, N., Oono, E., Baika, T., Sanda, S. "Effectes of a Prechamber on NOx Formation Process on the SI Engine. SAE Paper 790389-1979.
- (6) Matsuoka, S., Kawakita, T., Oguri, A., Tasaka, H. "A New Concept Three Valve, Pre-Chamber SI Engine is functioned by Three Stage Combustion Mechanism." FISITA-17th, BUDAPEST, p-1379~1394, 1978.
- (7) Tasaka, H., Yamamoto, H., Matsuoka, S. "Heatloss and Heat Release of Sub-Chamber SI Engine. Trans-JSME Vol-51-467, 1985.
- (8) Murata, H., Tasaka, H., Matsuoka, S., Igarashi, Y. "Measurement and Analysis of Non Uniform Gas Temperature Field in Tri-Valve SI Engine with Pre-Chamber. Trans-JSAE" Vol. 21-1980.
- (9) Tasaka, H., Matsuoka, S. "Gas Exchange Process of 4 cycle SI Engine under partial load and low or middle speed." T-JSME Vol. 40-335, 1974.
- (10) Khan, I. M., Greeves, G., Way, C. H. T. "Factors Affecting Soot and Gaseous Emissions from D.I. Engines and a Method of Calculations". SAE Paper No. 730169, 1973.
- (11) Matsuoka, S., Yoshizaki, T. "Model Verification of Burned Gas Re-Entrainment Phenomenon and the Soot Formation Mechanism in Diesel Combustion". T-SAE Vol. 98, Paper-890440 1989.
- (12) Tasaka, H., Mikogami, T., Matsuoka, S. "Heatloss and Heat Release of Pre-Mixed Combustion at a Constant Volume Bessel with Sub-Chamber". T-JSME Vol-50, 454-B 1984.
- (13) Matusoka, S., Katsuki, M. RC- 86 Intermittent Report 1990 JSME
- (14) Matsuoka, S., Sugimoto, G., Oda, N. RC-107 Intermittent Report 1993 JSME